Nonlinear Analysis on Prying of Top- and Seat-Angle Connections

Top- and seat angle 接合のてこ作用に関する非線形解析

Ali AHMED*, Norimitsu KISHI**, Ken-ichi MATSUOKA**, and Masato KOMURO***

アリ アハメド・岸 徳光・松岡健一・小室雅人

*Member Ph. D. Candidate, Dept. of Civil Engineering, Muroran Institute of Technology
**Member Dr. Eng., Prof., Dept. of Civil Engineering, Muroran Institute of Technology
***Member Dr. Eng., Res. Assoc., Dept. of Civil Engineering, Muroran Institute of Technology
(27-1 Mizumoto, Muroran 050-8585)

Nonlinear finite element (FE) analyses are performed to simulate the behavior of top- and seat-angle connections. Contact model with small sliding option is applied between contact pair surfaces of all connecting elements. Bolt pretension force is introduced in the initial steps of analysis. Numerical analysis results together with the prediction by Kishi-Chen power model are compared with experimental ones to examine the applicability of proposed analysis method and power model. The study is farther extended by analyzing the models varying connection parameters, material properties of connection assemblages, and magnitude of bolt pretension. The following results are obtained: 1) bolt sustains additional tensile force due to prying action; 2) prying force develops more quickly due to increment of bolt diameter, gage distance from angle heel to the centerline of bolt hole, and reduction of angle thickness; and 3) bolt pretension increases the initial connection stiffness.

Key Words: semi-rigid connection, finite element method, moment-rotation behavior, prying action.

1. Introduction

Semi-rigid connection has become more common in the area of steel frame analysis and design because of belonging a large number of steel beam-to-column connections to this type. With reference to practical application of semi-rigid steel frame construction, a new regrouping of semi-rigid connections was adopted in AISC-LRFD specification (1994) as PR (partially restraint) construction. Despite recognition of PR construction, design guidelines for the semi-rigid connections have not been provided. It is mainly because of a lack of adequate understanding on the behavior of semi-rigid connections in deferent aspects. One of such difficult measures is to determine the actual stress and deformation patterns of beam-to-column connections. Commonly, in the experimental test, stresses in the connection elements are estimated by converting the values of strain found in them. However, it is not an easy task to measure the actual strain and deformation in experimental test, which are necessary for predicting stress-deformation patterns of connections. In contrast, with the availability of more sophisticated computational and analytical tools, researchers are able to execute more realistic and rational analysis of semi-rigid beam-to-column connections. This development is reflected in the evolution of modern specifications.

To predict moment-rotation behavior of beam-to-column connections, several experimental studies (Azizinamini et al. 1985, Harper 1990, and others) had been performed. Many researchers have used these experimental works to examine the validity of their analytical studies, which were performed largely for developing a mathematical expression linking connection details to the moment-rotation (hereinafter, $M-\theta_r$) curves. Among those formulations, Frye-Morris' polynomial model (1975) and Kishi-Chen's power model (1990) are most potential ones. However, most of these analytical formulations exist with some shortcomings. Kishi-Chen proposed a three-parameter power model (1990), which becomes familiar for its easy application in second-order frame analysis using semi-rigid connections. But, the stiffness and pretension of bolts are not considered in that model to predict the respective ultimate moment capacity and initial connection stiffness.

As a category of semi-rigid connections, top- and seat-

Table 1 Geometrical properties of FE analysis model

FE model	Column section	Beam section	Top and seat angles					Bolt diameter d_b (mm)
			Angle section	Length L (mm)	Gage on column flange g (mm)	Bolt spacing on column flange p (mm)	Bolt spacing on beam flange s (mm)	
A1, A1np FE5, FE6	W12×96	W14×38	2L6×4×$^3/_8$	203	64	140	89	22
A2, A2np FE8, FE8np			2L6×4×½		64			
FE1, FE1np FE7, FE7np			2L6×4×¾					
FE2, FE2np			2L6×3½×$^3/_8$		51			
FE3, FE3np			2L6×6×$^3/_8$		114			
FE4, FE4np			2L6×4×½		64			19

For models A1, A2, FE1~FE8 bolts pretension is considered in the analysis;

For models A1np, A2np, FE1np~FE4np, FE7np, FE8np no pretension in bolts is considered in the analysis;
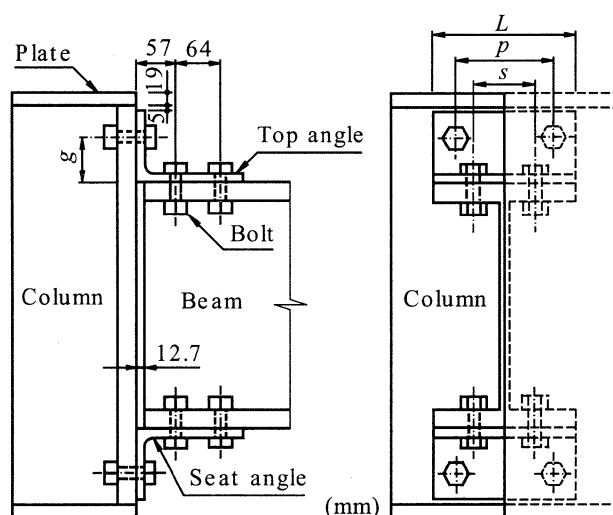

Fig. 1 Top- and seat-angle connection

angle connection is studied in this phase. A view of the connection is shown in Fig. 1. Basically, this type of connection is designed to transfer the vertical reaction of beam to column using the seat angle and to provide lateral support of the tension flange of beam using the top angle. However, based on the experimental results, it is seen that this type of connection is also able to transfer the end moment of beam to column partially.

Fleischman (1988) and Chasten et al. (1989) had experimentally investigated the behavior of connection's components to observe the effect of prying action on tension bolts. Those studies reveal that interaction between top angle and column flange causes additional tension in bolts due to prying action, which depends on connection parameters: bending stiffness of bolts and top angle, and location of connecting bolts; and which causes a substantial reduction of ultimate strength of bolts.

In this study, in order to precisely investigate the interaction between the column flange and the top angle's vertical leg accompanying with the affection of bolt action on M-θ_r characteristics of connection, nonlinear FE analyses are performed. To summarize, first of all, the applicability of proposed FE analysis method and power model by Kishi and Chen (1990) on static moment-rotation behavior of connection are assessed comparing with the experimental results. Following that the elasto-plastic behaviors of connection and connecting elements are investigated by analyzing FE connection models varying connection parameters and magnitude of pretension force introduced in the bolts.

2. Connection Model

2.1 Geometries of Connection Models

Geometrical properties of connection models for FE analysis are listed in Table 1 accompanying with column and beam sections. Each variable connection parameter listed in Table 1 is shown in Fig. 1. The other connection parameters are kept constant among all connection models and these are also depicted in the same figure. In the table, first two models are used for confirming the applicability of proposed FE technique. The models nominated as 'A1' and 'A2' are taken from the experiments of Azizinamini et al., (1985). The

Table 2 Material properties used in FE analysis

FE model	Angle		Bolt	
	Yield stress $\sigma_{y,a}$ (MPa)	Ultimate strength $\sigma_{u,a}$ (MPa)	Yield stress $\sigma_{y,b}$ (MPa)	Ultimate strength $\sigma_{u,b}$ (MPa)
A1, A2, FE1~FE6, A1np, A2np, FE1np~FE4np	365	550	635	830
FE7, FE7np	250	400		
FE8, FE8np	365	550	830	1035

connection models nominated by adding 'np' with corresponding preceding designation are the cases of bolt pretension ignored. All columns and beams in connection models used for parametric study are the respective sections of W12 × 96 and W14 × 38, for which geometrical measurements are taken from AISC-LRFD specifications (1994). As a mesh configuration example, a half model of A2 specimen is shown in Fig. 2. The total numbers of elements and nodes defined for model A2 are 10,330 and 17,984, respectively. Bolts in this model are more precisely constructed using eight node solid elements dividing into shank, head and nut elements to consider their individual affections on connection behavior. The bolt hole is formed 1.6 mm ($\frac{1}{16}$ in.) bigger than the bolt diameter according to the experiments by Azizinamini et al., (1985). The mesh pattern of a bolt is depicted in Fig. 3.

2.2 Material Properties

Material properties of angle and bolt are listed in Table 2. The properties of angle for all connection models except models FE7 are the same, which are taken from the test data of Azizinamini et al., (1985). To investigate the effects of material properties of angle on prying action, properties for model FE7 are assumed as the nominal values of A36 steel. Yield stress and ultimate strength of beam and column of all connection models are assumed the respective values of 365 MPa and 550 MPa. Material properties for bolts of all connection models except model FE8 are assumed as the nominal values of A325 bolts and for model FE8 are assumed as the nominal values of A490 bolts based on AISC-LRFD specifications because no coupon test results were reported in the experimental test data. A bi-linear elasto-plastic stress-strain relation with isotropic hardening rule for plastic deformation of all connection members is assumed taking Young's modulus E - 206 GPa and Poisson's ratio $\nu = 0.3$, in which strain hardening constant is determined assuming that the ultimate strain for bolts is 10% and for the other

connection members is 20%.

When moment-rotation curves of the connections are

Number of elements = 10,330
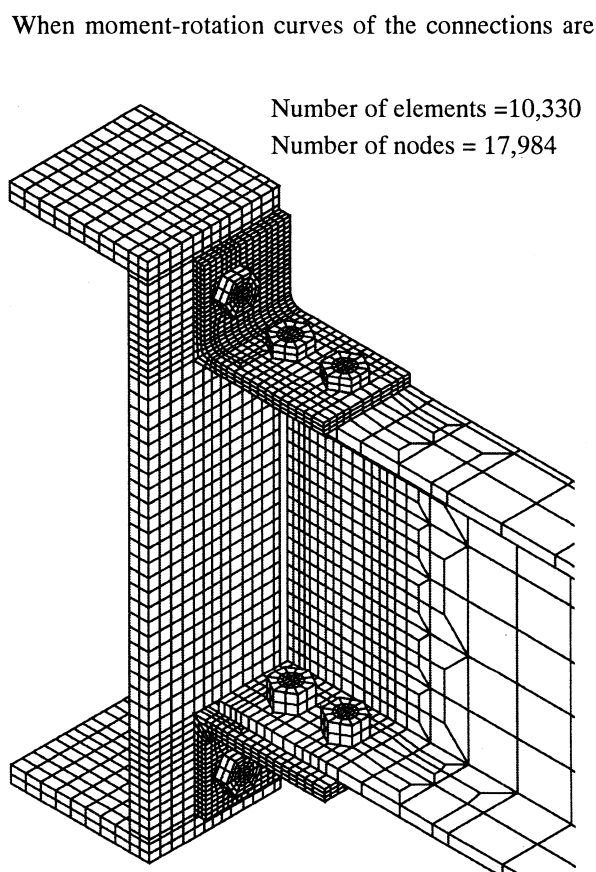Number of nodes = 17,984

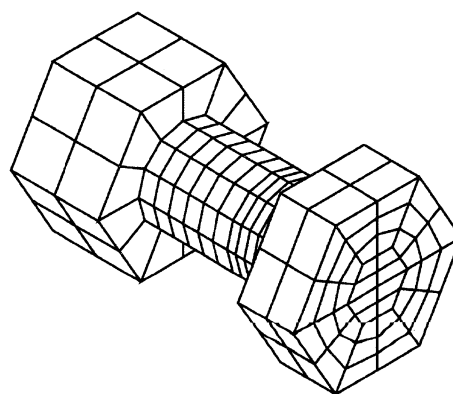Fig. 2 Mesh pattern of FE connection model A2

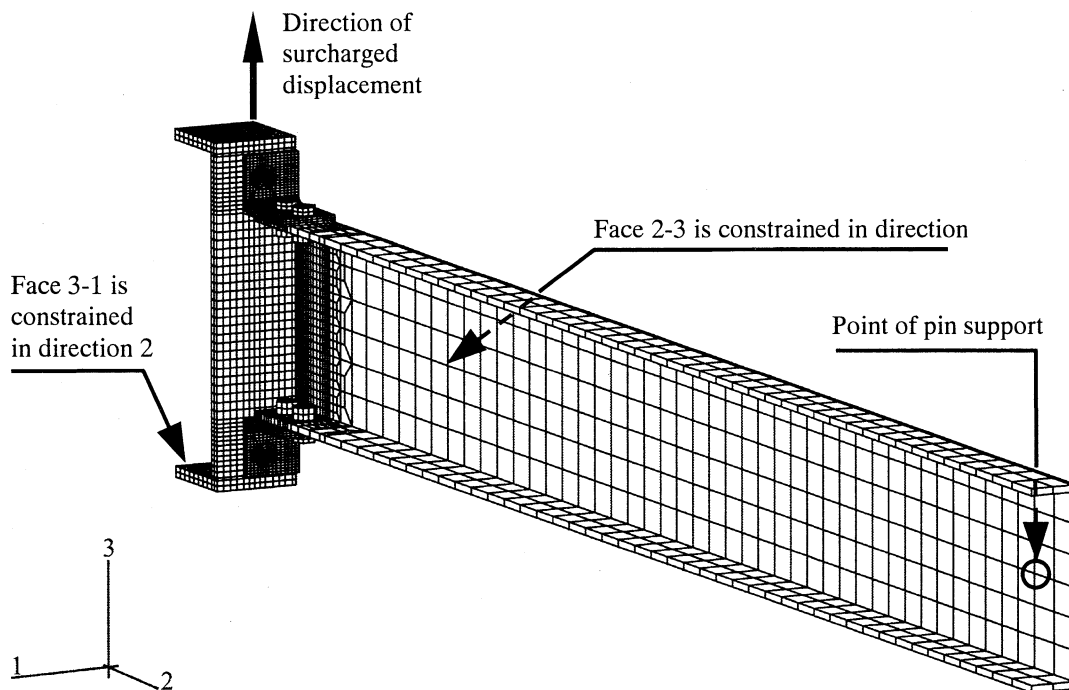Fig. 3 Mesh pattern of bolt of FE model A2

Fig. 4 Boundary conditions of FE analysis model

predicted by power model, angles are treated as perfectly elasto-plastic material, and bolts are as rigid body for simple design calculation.

3. Analytical Procedure

Numerical analyses of all connection models are performed using ABAQUS standards (1998) developed based on Finite Element Methodology. All components of a connection are modeled using first-order eight-node solid elements, which are pertinent to finite displacement and elasto-plastic structural analysis problems. Here, pretension force of bolts for all connection models except models A1np, A2np, FE1np through FE4np, FE7np, FE8np, FE5, and FE6 is prescribed up to 40 % of the ultimate strength of bolt, and for connection models FE5 and FE6 is 20% and 60% of that, respectively. All the connection models designated adding letters 'np' listed in Table 1 are also analyzed ignoring bolt pretension. The numerical results on the models without pretension of bolts are used to estimate prying force in the models with pretension of bolts.

FE models are analyzed following the experimental setup and loading method of Azizinamini et al., (1985), in which 1) two beams are symmetrically connected to the column flanges, 2) the ends of these beams are simply supported, and 3) letting the center of bottom surface of stub column move upward so that the forces corresponding to the prescribed bending moment can be distributed among the connection assemblages. Based on

these experimental boundaries, one-quarter model of connection composed of stub column, beam, top and seat angles and bolts is used for numerical analysis considering structural symmetry. Figure 4 shows a FE analysis model illustrating boundaries mentioned above. The FE analyses considering pretension force in bolts are performed in following three loading steps. In the first step, a pressure equivalent to prescribed pretension force is applied to the pre-defined section of bolt shank. As a result, the length of bolt shank at the pretension section changes by the amount necessary to carry the prescribed load. In the second step, the prescribed load in bolt is replaced by changing the length of pretension section back to the initial length. In the third step, bending moment is introduced to the beam-to-column connection by employing vertical displacement of the middle section of plane 3-1 of stub column.

To precisely analyze the behavior of connecting elements, contact pair model with small sliding option is applied against the contact surfaces between the vertical leg of angle and column flange, between the horizontal leg of angle and corresponding beam flange, and between the bolt and bolt hole elements. Moreover, to consider the frictional force, Coulomb's coefficient is assumed as 0.1 in the contact pair model.

4. Results and Discussions

4.1 Applicability of FE Method and Power Model

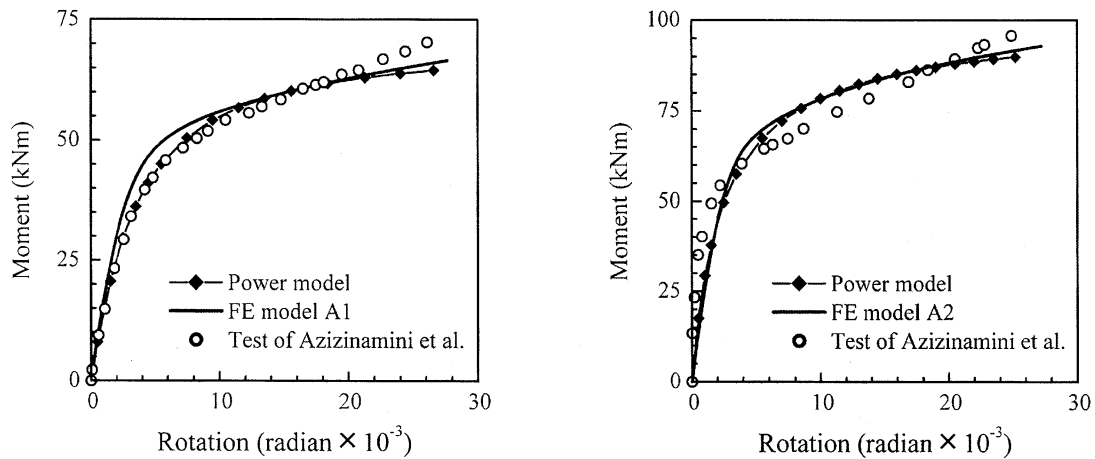First of all, to examine the applicability of FE analysis

Fig. 5. Comparison of $M-\theta_r$ curves predicted by FE analysis and power model with experimental results

method used for simulating elasto-plastic behavior of top- and seat-angle connections, numerical analyses for two connection specimens are performed and those numerical results together with the prediction of Kishi-Chen power model (1990) are compared with the experimental ones. The experimental results reported by Azizinamini et al., (1985) are used for the comparison. Following the experiments, a prescribed pretension force that is 40% of the ultimate strength of bolt is considered for all bolts in the connection. The comparisons of $M-\theta_r$ curve among analytical and experimental results are shown in Fig. 5. These comparisons reveal that FE analysis results and power model prediction curves are almost identical to the experimental curves in the linear elastic and early plastic ranges. However, both models show more flexible behavior than test connection in the large rotation area. The differences among the three results in the plastic range can be caused by the following reasons: 1) in FE analysis, yield plateau and nonlinear plastic behavior of angles and bolts are not considered; 2) in power model, bolts are assumed to be perfectly rigid body, and the locations where plastic-hinges are formed in angles are logically fixed; and 3) any experimental error may occur during the test. Even though analytical results differ a little from experimental ones, the FE analysis method still can be applied to investigate the effect of connection parameters on prying action, and power model has a potential of predicting $M-\theta_r$ curves of top- and seat-angle connections satisfactorily.

4.2 Stress-Deformation Behavior of Connection

Figure 6 shows the deformation configuration at the ultimate state of connection model A2. The figure shows that although the horizontal maximum displacement is occurred at the heel of top angle, the vicinity of the bolt hole of top angle's vertical leg is deformed severely.

Figure 7 shows the Mises stress contour at the ultimate state of model A2, in which connection moment is 103.5 kNm. From this figure, it is made clear that comparatively higher stresses develop near the bolt hole and fillets of top angle. The bending moment generated from the reaction force developed at the beam end support is converted to tension and compression forces in the connection, which are transferred to the column flange through the bolts fastening the angles to the column flange. The bolts are elongated due to the bending-tension force introduced by the top angle, and the top angle's vertical leg behaves as a lever supported in the area from the lower portion of bolt hole through the top edge. As a result of interaction among top angle,
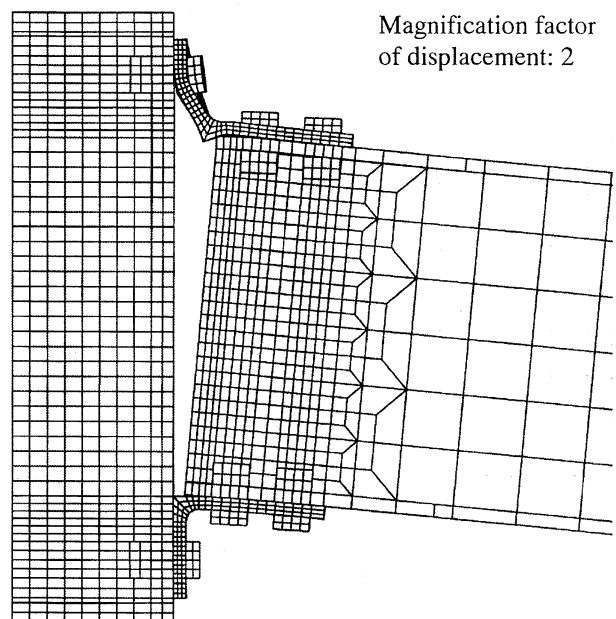

Magnification factor of displacement: 2

Fig. 6 Deformation configuration of connection model A2 at ultimate state

Mises (MPa)
+ 0.564
+ 56.00
+ 118.0
+ 179.0
+ 241.0
+ 303.0
+ 365.0
+ 426.0
+ 488.0
+ 550.0
+ 612.0
+ 673.0
+ 735.0
+ 1210.
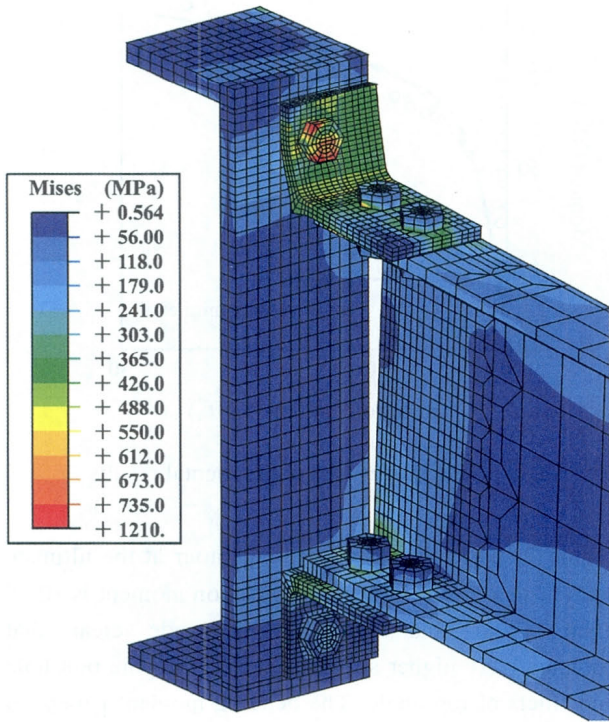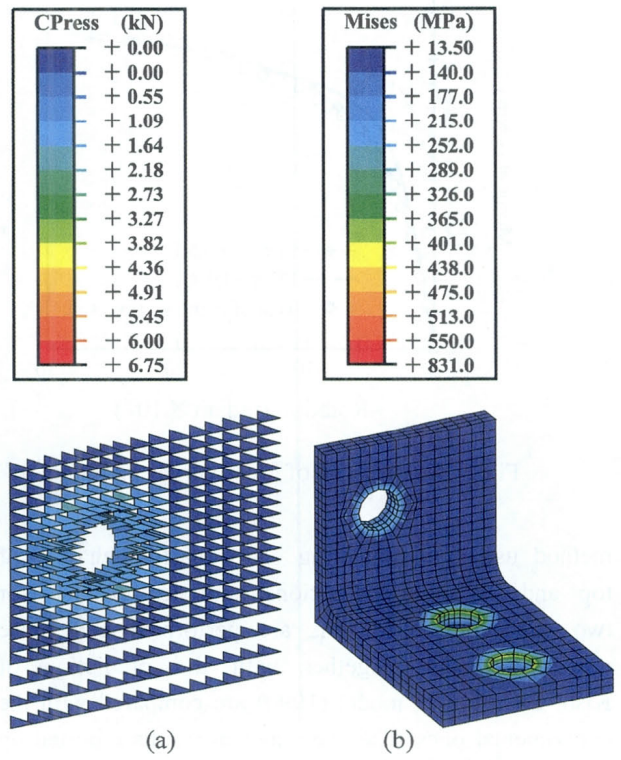
Fig. 7 Mises stress contour at ultimate state of model A2

(1) After pretensioning of bolts of A2

Stress σ_{22} (MPa)
− 852.0
− 635.0
− 502.0
− 369.0
− 235.0
− 102.0
+ 30.90
+ 164.0
+ 297.0
+ 430.0
+ 564.0
+ 697.0
+ 830.0
+ 1000.

(2) At ultimate state of model A2

(3) At ultimate state of model A2np

3
1   2

Fig. 8 Normal stress σ_{22} contour of tension bolt

CPress (kN)
+ 0.00
+ 0.00
+ 0.55
+ 1.09
+ 1.64
+ 2.18
+ 2.73
+ 3.27
+ 3.82
+ 4.36
+ 4.91
+ 5.45
+ 6.00
+ 6.75

Mises (MPa)
+ 13.50
+ 140.0
+ 177.0
+ 215.0
+ 252.0
+ 289.0
+ 326.0
+ 365.0
+ 401.0
+ 438.0
+ 475.0
+ 513.0
+ 550.0
+ 831.0

(a)   (b)

(1) Just after introducing pretension in bolts of model A2

(a)   (b)

(2) At ultimate state of connection model A2

(a)   (b)

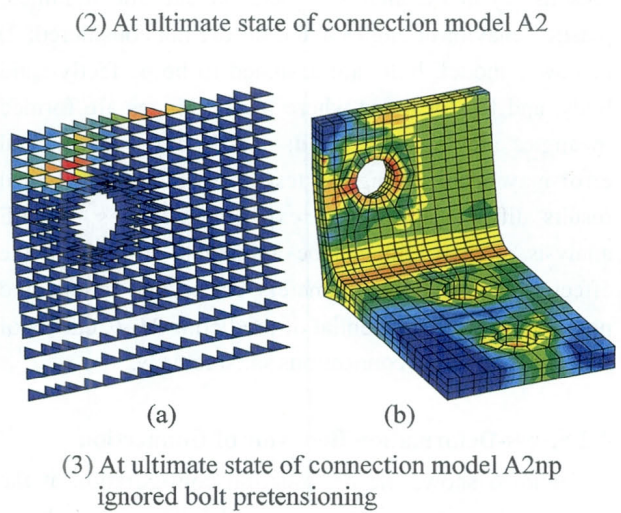(3) At ultimate state of connection model A2np
ignored bolt pretensioning

Fig. 9 (a) Contact pressure distributions on vertical leg of
top angle; (b) Mises stress contour of top angle

column flange and bolts, a reaction pressure is developed in the area from the centerline of bolt hole through the top edge. To keep the forces acting in the top angle in equilibrium state, bolts are loaded by an equal additional tensile force corresponding to the reaction pressure. The reaction pressure developed on vertical leg can be substituted by a resultant that is known as prying force. So, the tension bolts are loaded by not only pretension and bending-tension forces but also prying force.

Figure 8 shows the normal stress distribution patterns of σ_{22} caused in the tension bolt for model A2 and Fig. 9 illustrates: 1) nodal force distributions due to the contact pressure caused on the back surface of top angle's vertical leg (Fig. 9a); and 2) von Mises stress distributions of the top angle (Fig. 9b). The illustrations in Figs. 8 and 9 are focused on two cases: 1) one is for model A2 with pretension of bolts; and 2) the other is for model A2np without pretension of bolts. Figures 8 and 9 also depict the numerical results for two loading steps: 1) at the initial step after pretension force being introduced in the bolts (Figs. 8.1 and 9.1); and 2) at the ultimate state of connection (Fig. 8.2, 8.3, 9.2 and 9.3).

It is obvious from Figs. 8.1 and 9.1 that corresponding to the pretension force introduced in the bolts, the tensile stresses uniformly distribute in the whole bolt shank except the areas near bolt head and nut; in which low stress concentration occurs through the whole section of these regions (Fig. 8.1). And contact pressure is almost uniformly developed on the top angle's leg under the bolt head by the bolt tightening force.

At the ultimate state in both cases (Figs. 8.2 and 8.3), the stress in the whole area of bolt shank is over the yielding point ($\sigma_{y,a}$ = 365 MPa). Especially, the stress in the lower area of the bolt shank near the bolt head reaches the ultimate level ($\sigma_{u,b}$ = 830 MPa), and the upper area is under the compressive stress higher than the yielding point ($\sigma_{y,b}$ = 635 MPa). It can be observed in Figs. 9.2a and 9.3a that the contact nodal forces are more concentrated at the upper area of the left-hand side of vertical leg while the connection moment is increased up to the ultimate state. At this stage, the distributions of contact nodal forces on top angle's vertical leg and Mises stress in the top angle for both models A2 and A2np are similar to each other. This evident reveals that prying force and Mises stress distribution of top angle are obtained similar values for the both cases (with and without pretension of bolts) and are not affected by the magnitude of pretension force of bolts at the ultimate state of connection.

The power model is practically formulated simply by assuming that 1) angles are perfectly elasto-plastic body; 2) bolts are perfectly rigid body; and 3) connection

behaves two-dimensionally like a beam. The plastic-hinges in the top angle at the ultimate state of connection assumed by Kishi and Chen (1990) are shown in Fig. 10. It is evident from Figs. 9.2b and 9.3b that the yielded area in the top angle estimated by FE analysis are around the locations of plastic-hinge assumed by Kishi and Chen in the power model. Since FE analysis results show that the stresses higher than the yielding point are generated in the bolt shank near the bolt head (Fig. 8.3), the nonlinear behavior of connection obviously differs from some assumption of power model.
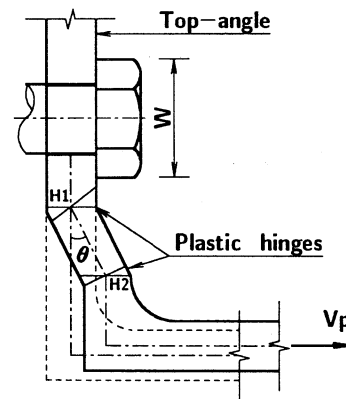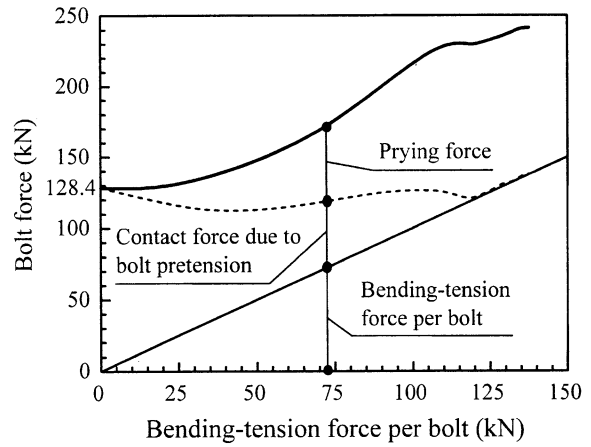

Fig. 10 Top angle failure mechanism
of power model

4.3 Distribution of Forces in Tension Bolt

ABAQUS standards are able to estimate the pressure occurred at each node of contact surface between top angle and column flange, and their resultant force, which is necessary for determining prying distribution on bolt tension force. Figure 11a shows the distribution between total tension force surcharged to bolt and bending-tension force per bolt in case of model A2np, in which bolt pretension is ignored. It can be observed from this figure that tension force of bolt is almost one and half time as much as bending-tension force up to near the ultimate state. If the bending stiffness of top angle were infinite, tension force of bolt would be equal to bending-tension force. So, it is obvious that excess tensile force in bolt is added by the prying force, which is caused by the deformation of top angle's vertical leg. It is apparent that prying force in connection models with pretension of bolts is also introduced in the tension bolt. However, it is too difficult to estimate the prying force subjected to the bolt because bolt force consists of three components: bending-tension force, contact force due to bolt pretension force, and prying force. In this study, it is assumed that the distribution of prying force corresponding to the bending-tension force is similar to that for the case without pretension of bolts. Figure 11b
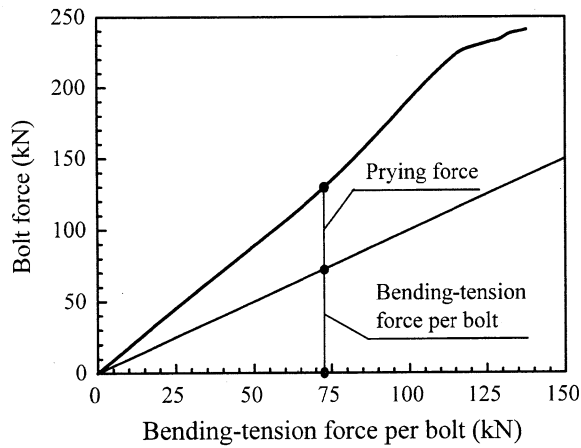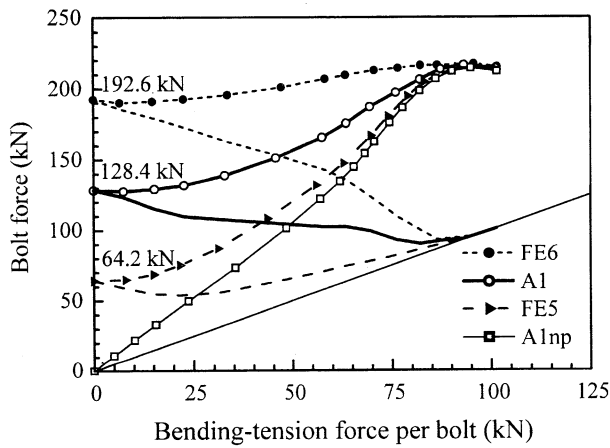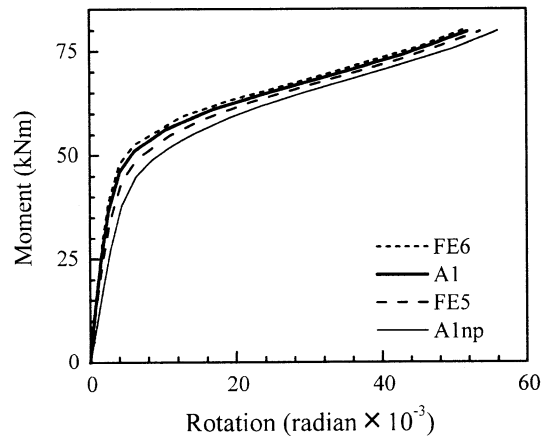
(a) FE analysis model A2np   (b) FE analysis model A2

Fig. 11 Prying phenomenon on bolt force

(a) Pretension effect on prying   (b) Pretension effect on $M-\theta_r$ curves

Fig. 12 Bolt pretension effect on prying and moment-rotation characteristics

shows the distribution of forces in tension bolt of model A2. It is seen that three components of bolt force can be properly estimated. From this figure, it is observed that the component of contact force caused by pretensioning bolts is decreased not linearly but nonlinearly with increasing bending-tension force of connection.

4.4 Effects of Bolt Pretension on Prying and Connection Behavior

Figure 12 shows the comparison of distributions of bolt force and $M-\theta_r$ curves among four models considering different ranges of pretension force in bolts. These models are A1np, FE5, A1, and FE6 of which pretension forces are 0%, 20%, 40%, and 60% of the ultimate state of bolt, respectively, and all the other conditions are similar among them. It can be observed from Fig. 12a that bolt tension forces for corresponding models started from different stages become closer among them, and prying force near the ultimate state is

not affected by the magnitude of pretension force. At the higher loading stage, contact force due to pretensioning bolts is eradicated entirely and only prying force is remained. From Fig. 12b, it is seen that initial connection stiffness is not much affected by the pretension force of bolt, and the ultimate moment capacity is almost the same among four cases, which can be converted from bending-tension force. Thus, it is made clear that $M-\theta_r$ curve of connection is hardly affected by the pretension force of bolt.

5. Influence of Connection Parameters on Prying Force

5.1 Bolt Diameter

Many alike Kishi and Chen (1990) disregarded the bolt stiffness in their mathematical model of predicting $M-\theta_r$ characteristics of connections. To investigate the

effect of bending stiffness of bolt on prying force, numerical analyses are performed for two connection models FE4 and A1, of which bolt diameters (d_b) are taken 19mm (¾ in.) and 22mm (⅞ in.), respectively, and pretension force is 40% of the ultimate strength of bolt. The effect of bolt size on bolt force is depicted in Fig. 13. At the beginning of loading, prying force grows very similarly in both connection models, but near ultimate state, connection model with bigger bolt diameter develops higher prying forces.

5.2 Angle Thickness

As it is recognized that thickness of top angle is one of the most influential parameters for representing connection behavior, its influence on prying action is also studied. Respective thicknesses (t_t) of connection models A1, A2, and FE1 are 9.5 mm (⅜ in.), 12.7 mm (½ in.), and 19.1 mm (¾ in.), and their other geometrical properties including bolt diameter (22 mm) are the same. It is observed from Fig. 14 that bolt tension force in model A1 increases most rapidly among the three models. It occurs because prying force develops faster for lesser thickness of angle.

5.3 Gage Distance

The gage distances on top angle's vertical leg from the heel to the centerline of bolt hole (g) are taken as variable. Those are 51mm (2 in.), 64mm (2.5 in.) and 114mm (4.5 in.) for connection models FE2, A1 and FE3, respectively, with common connection parameters: angle thickness 9.5 mm (⅜ in.) and bolt diameter 22 mm (⅞ in.). It is evident from Fig. 15 that prying force increases rapidly in connection with larger gage distance.

5.4 Material Properties of Angle and Bolt

The influences of material properties of angle and bolt on prying action are obviously depicted in Figs. 16 and 17, respectively. It is observed from Fig. 16 that prying force for connection model FE7 with weaker angles (yield stress, 250 MPa and ultimate strength, 400 MPa) develops a little greater than that for connection model FE1 with stiffer angles (yield stress, 365 MPa and ultimate strength, 550 MPa). On the other hand, Fig. 17 demonstrates that the material properties of bolt have no effect on prying action throughout the complete loading history excluding near the ultimate loading stages. Connection model FE8 with stiffer bolts (yield stress, 830 MPa and ultimate strength, 1035 MPa) exhibits a little bigger prying force than the connection model A2 with weaker ones (yield stress, 635 MPa and ultimate strength, 830 MPa).
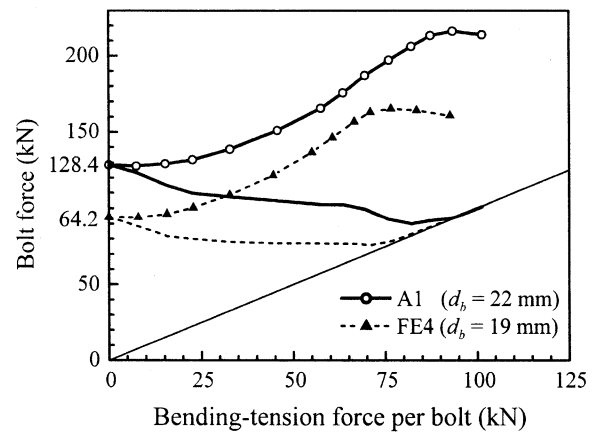

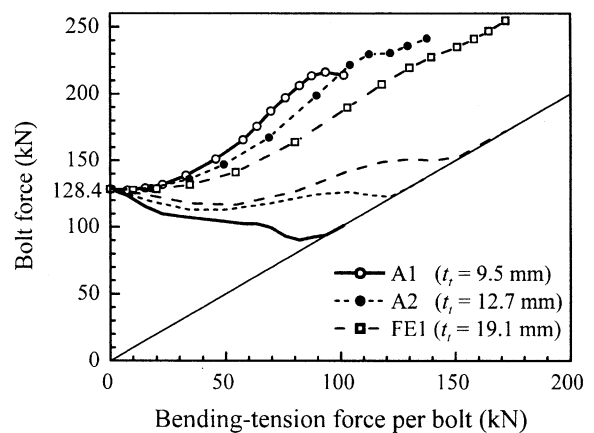Fig. 13 Bolt diameter effect on prying force
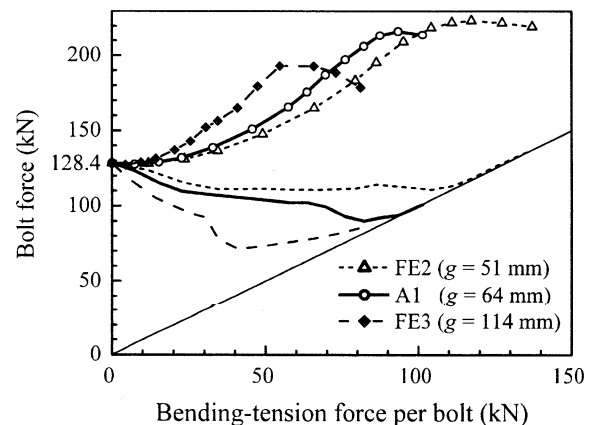

Fig. 14 Influence of angle thickness on prying

Fig. 15 Influence of gage from angle heel to bolt hole centerline on prying force

6. Concluding Remarks

In order to precisely investigate the interaction between the column flange and the top angle's vertical leg on $M-\theta_r$ characteristics of top- and seat-angle connections, nonlinear FE analysis was performed. The

applicability of FE analysis results was verified comparing with experimental results. It is confirmed from the comparison that nonlinear connection behavior of top- and seat-angle connections accompanying with large deformation can be analyzed by using proposed FE analysis technique taking pretension force of bolts, and contact and sliding effects of connecting elements into account. In addition, an applicability of three-parameter power model with semi-analytical formulation was also verified comparing with experimental as well as the numerical results of FE analyses. This study interprets that power model is able to predict $M-\theta_r$ curves of the connection satisfactorily and can be applicable of doing nonlinear analysis of steel frames with semi-rigid connections.

Confirming about the applicability of FE analysis model, a parametric study was also conducted varying dimensions of connection models and magnitude of pretension force surcharged to the bolts to investigate its affection on prying action. This investigation furnishes by the following conclusions:

(1) Pretension force of bolts has no effect on prying action at the ultimate state of connections.

(2) Reduction of flange angle thickness or increment of angle's gage distance on column flange can develop a larger prying force.

(3) Supplying of stiffer bolts or weaker angles in connection may cause more increase in prying force.

(4) Tension bolt and angle (especially of thin thickness) may reach early at the ultimate state due to the effect of prying action.
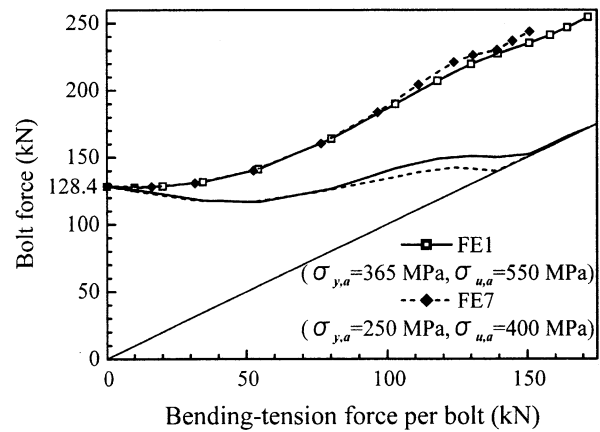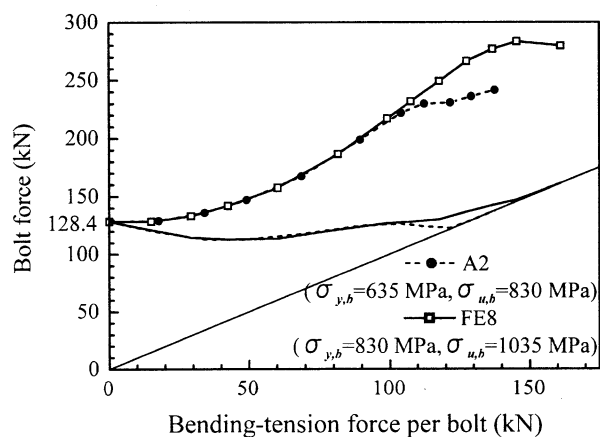

Fig. 16 Influence of material property of angle on prying force

Fig. 17 Influence of material property of bolt on prying force

REFERENCE

1) ABAQUS, Standard, *User's Manual*, Version 5.8, Vol.I- III, Hibbitt Karlsson & Sorensen, Inc., 1998.

2) American Institute of Steel Construction, *Manual of Steel Construction, Load and Resistance Factored Design, AISC,* Chicago, Vol.I & II(2), 1994.

3) Azizinamini, A., Bradburn, J.H. and Radziminski, J.B., Static and Cyclic Behavior of Semi-Rigid Steel Beam-Column Connections, *Structural research studies,* Department of Civil Engineering, University of South Carolina, Columbia, S.C., March, 1985.

4) Chasten, C.P., Fleischman, R.B., Driscoll, G.C. and Lu, L.W., Top-and-Seat-Angle Connection and End-Plate Connections: Behavior and Strength under Monotonic and Cyclic Loading, *Proc. of National Engineering Conference,* American Institute of Steel Construction, Chicago, Vol.3, pp.6-1-6-32, 1989.

5) Fleischman, R.B., Experimental and Theoretical Analysis of Component Behavior in Top-and-Seat--Angle Connections, *ATLSS Project A3.1,* Master's thesis, Lehigh University, Pittsburgh, PA, 1988.

6) Frye, M.J. and Morris, G.A., Analysis of Flexibly Connected Steel Frames, *Canadian Journal of Civil Engineers,* Vol.2(3), pp.280-291, 1975.

7) Harper, W.L., Dynamic Response of Steel Frames with Semi-Rigid Connections, *Structural research studies,* Department of Civil Engineering, University of South Carolina, Columbia, S.C., May, 1990.

8) Kishi, N. and Chen, W.F., Moment-Rotation Relations of Semi-Rigid Connections with Angles, *Journal of Structural Engineering, ASCE,* Vol.116(7), pp.1813-1834, 1990.